

Physics Analysis on the NRU Core for an Accident Scenario of a Loop Pressure Tube Crack

T.C. Leung

Chalk River Laboratories,
Atomic Energy of Canada Limited, Chalk River, Ontario K0J 1J0, Canada
leungt@aecl.ca

Abstract

The Nuclear Research Universal (NRU) reactor loops are high temperature, high pressure test facilities, designed for power reactor fuel development and materials testing within the core of the NRU reactor. The loops allow test material to be subject to neutron flux, temperature and pressure conditions typical of a power reactor. This paper describes the physics analysis on the NRU core for an accident scenario of a loop pressure tube crack with a concurrent liner tube failure. After the crack has occurred, thermal-hydraulic analysis predicts the formation of a steam bubble of 50 cm radius in the D₂O moderator/coolant around the loop test section. The steam displaces the D₂O moderator and has a negative reactivity effect. This negative reactivity effect is large enough to overcome the positive loop void reactivity such that the reactor is shut down and reactor safety is not compromised. The paper also describes the sensitivity of steam bubble densities on the reactivity effect and presents results for subsequent reductions of fluxes and channel powers around the loop site.

1. Introduction

The Nuclear Research Universal (NRU) reactor at Chalk River Laboratories began operation in 1957. It is used to carry out research in basic science and in support of the CANDU[®] power reactor program. It is also a major supplier of medical radioisotopes in Canada and the world. The NRU reactor is heavy water cooled and moderated, with on-line refueling capability. It is licensed to operate at a maximum power of 135 MW, and has a peak thermal flux of approximately $4.0 \times 10^{18} \text{ n.m}^{-2}.\text{s}^{-1}$. The hexagonal lattice pitch between adjacent sites is 19.685 cm.

The NRU reactor loops [1] are high temperature, high pressure test facilities, designed for advanced power reactor fuel development and materials testing within the NRU reactor core. The U1 and U2 loops allow test material to be subject to neutron flux and temperature and pressure conditions typical of a power reactor. Figure 1 shows a typical loop fuel test site, which contains a fuel string with six vertical test fuel bundles on a common tie-rod. A severe accident to the NRU reactor may occur as a result of a loop pressure tube crack with a concurrent liner tube failure. This postulated accident has been analyzed by engineering and probabilistic safety assessment methods and classified as an incredible event, which is an event that has less than 1 in 10^6 probability of occurring.

CANDU[®] (CANada Deuterium Uranium) is a registered trademark of Atomic Energy of Canada Limited (AECL).

However, from the physics point of view it is important to assess the impact of the loop pressure tube and liner tube failure on the reactivity, flux and power changes of the NRU reactor core. After the pressure tube crack has occurred, a thermal-hydraulic analysis performed using the TUBRUPT-IST code [2] for a full-length crack of the NRU loop pressure tube predicts the formation of a spherical steam bubble of 50 cm radius in the D₂O moderator/coolant around the center of the loop test section. The bubble density may vary from 10 kg/m³ at 0.05 s. to 2 kg/m³ at 0.3 s. The analysis of using a steam bubble is conservative because the actual volume occupied by steam is expected to be larger. The steam displaces the D₂O moderator and has a negative reactivity effect on the reactor core. This paper describes the assessments of the reactivity effects and the resulting power changes on the NRU core due to the loop pressure tube crack. The paper also presents the physics analysis methodology and the key findings, including the sensitivity of the steam bubble densities on reactivity effects.

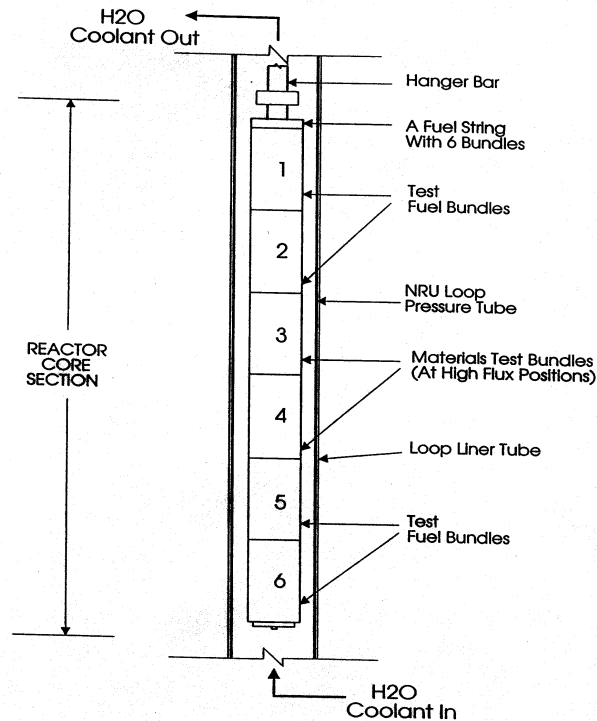


Figure 1 Schematic of a typical NRU loop fuel test site with a fuel string of 6 fuel bundles.

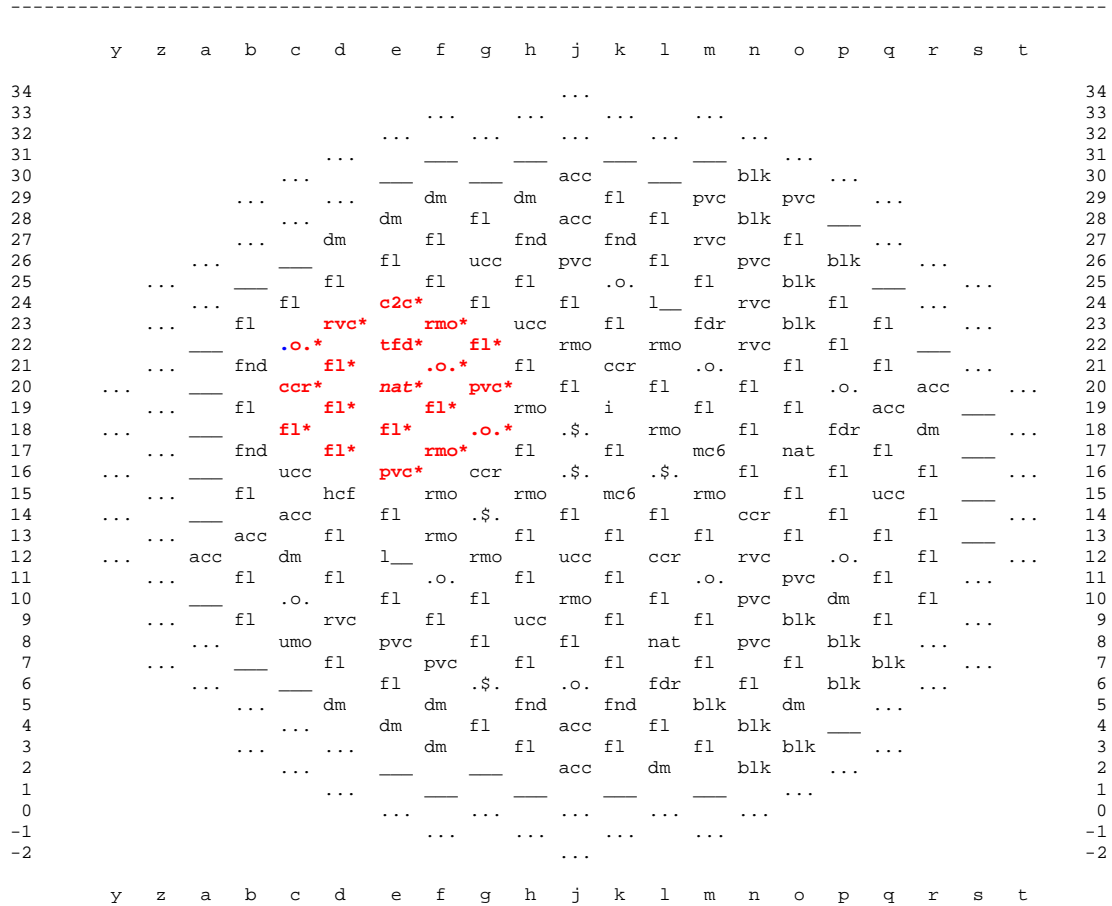
2. Analysis methodology

The analysis methodology included the following steps:

1. Establishing the initial NRU reference core loading for the analysis.
2. Determining the affected regions of the cores according to the size and volume of the steam bubble around the loop test section.
3. Generating the homogenized neutronic diffusion parameters of rod assemblies for the affected regions of the core.

4. Calculating the reactivity changes and the flux and power changes for the core affected by steam, using TRIAD3 [3], which is a validated reactor neutronic simulation code for NRU.

core loading - core k03g28



Legend:

| | | | |
|-----------------------|------------------------|--|---|
| fl =driver fuel rod | dm=dummy fuel rod | pvc=preferred vacant site | rvc=reserved vacant site |
| rmo=moly rod | fdr=flux detector site | blk=blocked | nat=loop with natural uranium fuel string |
| acc=accessible site | ccr=cobalt rod | ucc=cadmium rod | fnd=fast neutron rod dummy |
| ..., __=d2o site | mc6=multicapsule rod | umo=Umo fuel test site | hcf=hydraulic capsule facility |
| .\$.=control rod site | .o.=control rod site | c2c= d2o site with a small scattering-can at about mid-plane | tfd=traveling flux detector rod |

Note:- “*” refers to sites occupied by steam.

Figure 2 Core loading for the initial NRU reference core and regions affected by steam.

2.1 Establishing the initial reference core

Figure 2 shows the core loading of the initial reference core and regions affected by steam. The core used for this study was based on the NRU core loading of 2004 November 2, when both the U1 and U2 loops were operating. This core was modified to be the reference core after the three loop assemblies at the E20, O17 (U2) and L08 (U1) sites were replaced with fresh natural uranium fuel strings, and two fuel rod positions (sites K03 and G28) were changed to rebalance the power distribution. This core loading results in a relatively large positive loop void reactivity effect, and is judged to be a conservative loading for the purposes of this analysis.

2.2 Determining the regions of the core affected by steam

NRU sites are modeled as hexagonal prism cells in the TRIAD3 code. In the present analysis, the volume of steam that is simulated in the NRU core includes those sites that are within a cylinder around the E20 loop site, with a radius of 49.2 cm (2.5 lattice pitches) from the center of the loop and with an axial height of ± 50 cm above and below the center horizontal plane. This simulated steam bubble prism has approximately the same volume as the spherical steam bubble of 50 cm radius predicted from the TUBRUPT code.

In Figure 2, the sites that are affected by steam in the NRU core are identified. The steam bubbles occupy the 18 neighbouring sites within 2 lattice pitches away from the E20 loop site. Table 1 lists the axial locations of those cell types that have been affected by steam. In this table, both the cell type names for all the assemblies with and without steam are listed.

2.3 Generation of homogenized neutron cell parameters for the NRU cells with steam

The NRU cell parameters for the reactor diffusion calculations are determined using the WIMS-AECL code [4], which is a multi-group transport code with two-dimensional capabilities using the Pij collision probability method. The cell parameters are generated using the standard NRU super-cell model, illustrated in Figure 3. In this model, the neighbouring fuel rods outside the normal cell-of-interest are modeled as two fuel/D₂O rings located at radii of 19.2 and 38.9 cm from the center of the cell to provide the correct driving spectrum. The outer boron B-10 ring is to provide adjustment for the cell k_{eff} to be within ~ 20 mk of 1.000. The present super-cell model used in WIMS does not account for the heterogeneity of the core. However, the issue of the heterogeneity is addressed by the use of cell discontinuity factors (*cdf*) in the TRIAD core calculation to improve the radial neutron leakages between adjacent rods made up of different materials (see Appendix A).

The presence of light water steam in the NRU cells affects the generation of the 2-group homogeneous cell parameters in various ways. In general, it increases the thermal absorption cross section, reduces the moderation effect by displacing the heavy water in the cell, and also causes the neutron spectrum to be harder. This effect is discussed below.

Table 1 Cell types affected by steam in the NRU core. Bold italicized cell type names show those cells with steam.

| Axial Section | Distance From Centre (cm) | E20 Loop Site (nat) | Driver Fuel Rod Sites (fl) | D ₂ O Sites (.o.,pvc, rvc,c2c) | Cobalt Rod Site (ccr) | Moly Rod Site (rmo) | Flux Detector Rod Site (tfd) |
|---------------|---------------------------|------------------------------------|--|--|--|---|--|
| | | | 1 st lattice pitch sites: d19, d21, e18, f19. 2 nd lattice pitch sites, c18, d17, g22 | 1 st lattice pitch site: f21 2 nd lattice pitch sites, c22,d23,e16, e24,g18,g20 | 2 nd lattice pitch sites, c20 | 2 nd lattice pitch sites, f17, f23 | 1 st lattice pitch sites: e22 |
| 1 | 150.0 to 175.0 | slph_bn | ddm_an | dd2o_an | ddm_an | dmol_abn | dshr_an |
| 2 | 137.0 to 150.0- | <i>dl3unase</i> dl3unaae | ddm_an | dd2o_an | ddm_an | dmol_abn | dshr_an |
| 3 | 125.0 to 137.0 | <i>dl3unase</i> dl3unaae | dfl_de | dd2o_an | ddm_an | dmol_abn | dshr_an |
| 4 | 100.0 to 125.0 | <i>dl3unase</i> dl3unaae | dfl_de | dd2o_an | sccr_ai | dmol_abn | dshr_an |
| 5 | 75.0 to 100.0 | <i>dl3unase</i> dl3unaae | dfl_de | dd2o_an | sccr_ai | dmol_abn | dshr_an |
| 6 | 50.0 to 75.0 | <i>dl3unase</i> dl3unaae | dfl_de | dd2o_an | sccr_ai | dmol_abn | dshr_an |
| 7 | 38.0 to 50.0 | <i>dl3unase</i> dl3unaae | <i>dfl_sde</i> dfl_de | <i>dd2o_san</i> dd2o_an | <i>sccr_sai</i> sccr_ai | <i>dmolsbbn</i> dmol_bbn | <i>dshr_san</i> dshr_an |
| 8 | 25.0 to 38.0 | <i>dl3unase</i> dl3unaae | <i>dfl_sde</i> dfl_de | <i>dd2o_san</i> dd2o_an | <i>sccr_sai</i> sccr_ai | <i>dmolscbe</i> dmol_cbe | <i>dshr_san</i> dshr_an |
| 9 | 0 to 25.0 | <i>dl3unase</i> dl3unaae | <i>dfl_sde</i> dfl_de | <i>dd2o_san</i> dd2o_an | <i>sccr_sai</i> sccr_ai | <i>dmolsdbe</i> dmol_dbe | <i>dshr_san</i> dshr_an |
| 10 | -25.0 to 0 | <i>dl3unase</i> dl3unaae | <i>dfl_sde</i> dfl_de | <i>dd2o_san</i> dd2o_an | <i>sccr_sai</i> sccr_ai | <i>dmolsdbe</i> dmol_dbe | <i>dshr_san</i> dshr_an |
| 11 | -38.0 to -25.0 | <i>dl3unase</i> dl3unaae | <i>dfl_sde</i> dfl_de | <i>dd2o_san</i> dd2o_an | <i>sccr_sai</i> sccr_ai | <i>dmolsdbe</i> dmol_dbe | <i>dshr_san</i> dshr_an |
| 12 | -50.0 to -38.0 | <i>dl3unase</i> dl3unaae | <i>dfl_sde</i> dfl_de | <i>dd2o_san</i> dd2o_an | <i>sccr_sai</i> sccr_ai | <i>dmolsebn</i> dmol_ebn | <i>dshr_san</i> dshr_an |
| 13 | -75.0 to -50.0 | <i>dl3unase</i> dl3unaae | dfl_de | dd2o_an | sccr_ai | dmol_ebn | dshr_an |
| 14 | -100.0 to -75.0 | <i>dl3unase</i> dl3unaae | dfl_de | dd2o_an | sccr_ai | dmol_ebn | dshr_an |
| 15 | -125.0 to -100.0 | <i>dl3unase</i> dl3unaae | dd_de | dd2o_an | sccr_ai | dmol_ebn | dshr_an |
| 16 | -137.0 to -125.0 | <i>dl3unase</i> dl3unaae | dfl_de | dd2o_an | ddm_an | dmol_ebn | dshr_an |
| 17 | -150.0 to -137.0 | <i>dl3unase</i> dl3unaae | ddm_an | dd2o_an | ddm_an | dmol_ebn | dshr_an |
| 18 | -175.0 to -150.0 | slph_bn | ddm_an | dd2o_an | ddm_an | dmol_ebn | dshr_an |

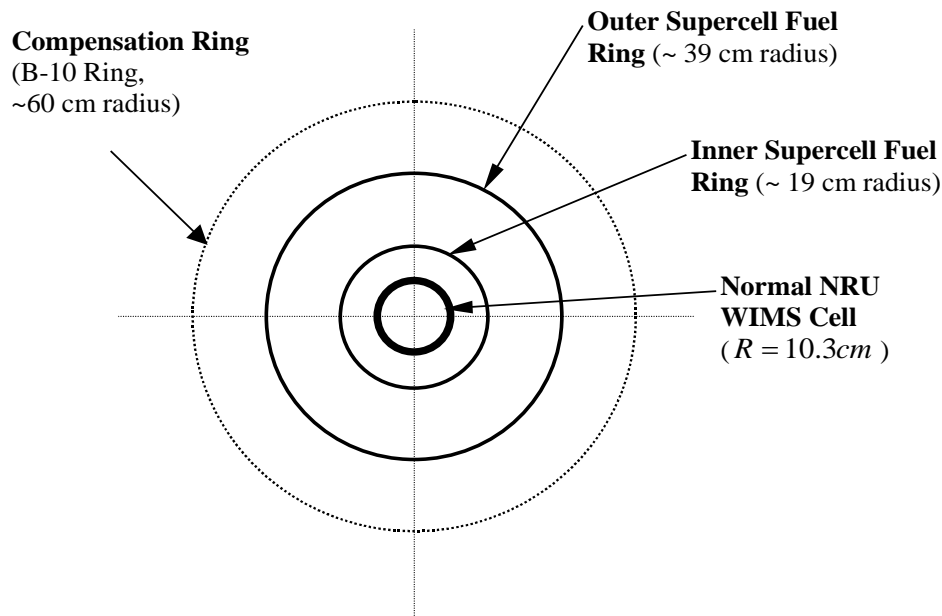


Figure 3 A supercell model for NRU.

The effects of steam on the cell parameters for the 18 rod assemblies within 2 lattice pitches around the loop have been assessed. As an example, the WIMS-AECL calculation results for an NRU driver fuel rod are shown in Table 2. In this table, the cell parameters for a cell with steam and without steam are compared, and the percent differences in each parameter are listed. An important effect of the presence of steam in the cell is the increase of the neutron absorption in the thermal groups, ~14%. This significantly overrides the 17% reduction in the fast group neutron absorption, which is only one-tenth of that in the thermal group. In general, the steam affects several key cell parameters of the neighbouring rods around the loop section and it has a net reduction effect on the neutron flux in this region of the core.

2.4 Calculation of reactivity, flux and power changes using the TRIAD3 code

The reactivity changes for the NRU core and the flux and power changes for those sites affected by steam were calculated using the TRIAD3 code. A general description of the TRIAD3 code is given in Appendix A. The different scenarios studied were as follows:

- Case 1 was for the initial reference core.
- Case 2 was for the core with loop voiding.
- Cases 3a and 3b were for the cores with steam occupying the full length of the E20 site, and also occupying the neighbouring 6 sites within 1 lattice pitch around the E20 loop test section between axial heights of ± 50 cm above and below the

- center horizontal plane. The steam bubble density was 10 kg/m^3 in Case 3a, and 2 kg/m^3 in Case 3b. In these two cases, calculations were performed to study the effect of a smaller size steam bubble of a radius of ~ 30 cm radius.
- Cases 4a and 4b were similar to Cases 3a and 3b, except that calculations were for a full size steam bubble of 50 cm radius. The steam occupies the neighbouring 18 sites within 2 lattice pitches around the loop test section between axial heights of ± 50 cm above and below the center horizontal plane. The steam bubble density was 10 kg/m^3 in Case 4a, and 2 kg/m^3 in Case 4b.

Table 2 Effect of steam on the two-group cell-parameters of NRU fresh driver fuel.

| Cell Parameters | Normal Cell Without Steam | Cell with Steam, Density = 10 kg/m^3 | Percent Change |
|--|---------------------------|--|----------------|
| Fission Cross Section (1), cm^{-1} | 0.2402E-03 | 0.1992E-03 | -17.07% |
| Fission Cross Section (2), cm^{-1} | 0.3043E-03 | 0.3417E-03 | +12.29% |
| Absorption Cross Section (1), cm^{-1} | 0.5237E-03 | 0.4307E-03 | -17.76% |
| Absorption Cross Section (2), cm^{-1} | 0.3916E-02 | 0.4503E-02 | +14.99% |
| Scatter Cross Section (1), cm^{-1} | 0.8664E-02 | 0.8637E-02 | -0.31% |
| Scatter Cross Section (2), cm^{-1} | 0.4163E-05 | 0.4120E-05 | -1.03% |
| Q-value (1), kW/cm | 0.2613E-14 | 0.2167E-14 | -2.07% |
| Q-value (2), kW/cm | 0.3310E-13 | 0.3717E-13 | +12.3% |
| <i>cdf</i> (1) | 0.7928 | 0.8859 | +11.74% |
| <i>cdf</i> (2) | 1.0744 | 1.0313 | -4.01% |

Note: (1)= fast group for neutron energy above 0.625 eV, (2)=thermal group for neutron energy below 0.625 eV.

In this study, the WIMS model accounts for the presence of steam in the "cell-of-interest", but not in the surrounding super-cell. Therefore, the overall effect of the present analysis is more conservative, because having steam in the super-cell will have further neutron reduction effect.

3. Results

3.1 Reactivity changes

The calculated results for the K_{eff} values for the initial core and other cores affected by steam are listed in Table 3. In general, the TRIAD3 code calculation produces slightly

high values of K_{eff} for critical core loadings by about 30 mk, due to approximations in the model, but is consistent and validated. For core loadings of recent years, the K_{eff} offset has increased to about ~50 mk, due to the decreasing heavy water isotopic concentration, which is not modeled. NRU has an on-line heavy water upgrading system, which will maintain the NRU heavy water purity to 99.85%, if it is operating properly.

From the first two cases in Table 3, the reactivity effect of voiding the E20 loop is +2.75 mk. This positive void reactivity is progressively reduced by the displacement of surrounding heavy water moderator by light water steam, which results in the loss of moderation and an increase in neutron absorption. For a smaller size steam bubble of ~30 cm radius displacing the moderator in the six neighbouring sites within 1 lattice pitch around the loop test section, the total net reactivity change is -0.56 mk, for a steam density of 10 kg/m³. Further increasing the steam bubble to a full radius of 50 cm into the 18 neighbouring sites within 2 lattice pitches from the loop test section provides a net reactivity change of -4.29 mk. With the steam bubble at a lower density (2 kg/m³), the reactivity effects are similar, although a little less negative. However, even for the case of lower steam density, the negative reactivity introduced by the full size steam bubble is sufficient to overcome the positive void reactivity (-2.91 vs +2.75 mk), and shut down the reactor.

Table 3 Summary of reactivity calculation results.

| Case No. | Core Description | K-effective (k_{eff}) | $1/k_{eff}$ | Change of $1/k_{eff}$ from Reference Core, |
|----------|---|---------------------------|-------------|--|
| 1 | Initial reference core | 1.046386 | 0.95567 | 0 |
| 2 | E20 loop completely voided, but with D ₂ O surrounding loop pressure tube | 1.049405 | 0.95292 | +2.75 mk |
| 3a | 6 neighbouring rods within 1 lattice pitch with steam (density =10 kg/m ³) | 1.045777 | 0.956227 | -0.56 mk |
| 3b | 6 neighbouring rods within 1 lattice pitch with steam (density =2 kg/m ³) | 1.046613 | 0.955463 | +0.21 mk |
| 4a | 18 neighbouring rods within 2 lattice pitches with steam (density =10 kg/m ³) | 1.041705 | 0.959965 | -4.29 mk |
| 4b | 18 neighbouring rods within 2 lattice pitches with steam (density =2 kg/m ³) | 1.043212 | 0.95878 | -2.91 mk |

3.2 Flux and power changes for neighbouring sites

Table 4 shows the comparisons of thermal fluxes for the 18 neighbouring sites within 2 lattice pitches from the E20 loop test section, for the cases with and without steam. In columns 3 and 5, the thermal fluxes are listed for the case with steam bubble density of

10 kg/m³, and of 2 kg/m³, respectively. The percentage reductions in the flux levels are shown in columns 4 and 6.

The reduction of fluxes varies with the rod types at different sites. The effect of flux reduction was the least for the cobalt rod at site C20, because the rod is a very strong neutron absorber. For the case of a steam bubble density of 2 kg/m³, there was a 1.4 % reduction for this rod site compared to a 13.4 % reduction for the average of the other 18 sites. The second least affected site by steam was a neighbouring fuel rod site next to the

Table 4 Comparisons of thermal fluxes for neighbouring sites around the loop with steam and without steam.

| Locations of Sites within the 2 nd Lattice Pitch, Site (rod type) | Thermal Fluxes For Sites With No Steam, x10 ¹⁴ n.cm ⁻² s ⁻¹ | Thermal Fluxes For Sites With Steam Density of 2 kg/m ³ x10 ¹⁴ n.cm ⁻² s ⁻¹ | Percent Change | Thermal Fluxes For Sites With Steam Density of 10 kg/m ³ x10 ¹⁴ n.cm ⁻² s ⁻¹ | Percent Change |
|--|---|--|-------------------|---|-------------------|
| D19 (fl) | 1.69 | 1.47 | -13.0% | 1.41 | -16.6% |
| D21 (fl) | 1.64 | 1.43 | -12.8% | 1.37 | -16.5% |
| E18 (fl) | 1.91 | 1.61 | -15.7% | 1.56 | -18.3% |
| E22(tfd) | 2.06 | 1.72 | -16.5% | 1.66 | -19.4% |
| F19 (fl) | 1.96 | 1.63 | -16.8% | 1.59 | -18.9% |
| F21(d ₂ o) | 2.14 | 1.73 | -19.2% | 1.68 | -21.5% |
| C18 (fl) | 1.49 | 1.39 | -6.7% | 1.33 | -10.74% |
| C20(ccr) | 1.44 | 1.42 | -1.4% | 1.35 | -6.25% |
| C22(d ₂ o) | 1.65 | 1.47 | -10.9% | 1.41 | -14.5% |
| D17 (fl) | 1.74 | 1.52 | -12.6% | 1.48 | -14.9% |
| D23(d ₂ o) | 1.93 | 1.62 | -16.1% | 1.58 | -18.1% |
| E16(d ₂ o) | 2.26 | 1.88 | -16.8% | 1.87 | -17.3% |
| E24(d ₂ o) | 1.91 | 1.74 | -8.9% | 1.70 | -11.0% |
| F17(rmo) | 2.13 | 1.82 | -14.5% | 1.80 | -15.5% |
| F23(rmo) | 2.01 | 1.75 | -12.9% | 1.71 | -14.9% |
| G18(d ₂ o) | 2.23 | 1.86 | -16.6% | 1.85 | -17.0% |
| G20(d ₂ o) | 2.26 | 1.86 | -17.7% | 1.83 | -19.0% |
| G22 (fl) | 1.86 | 1.63 | -12.4% | 1.60 | -14.0% |
| Average: | | | -13.4+4.2% | | -15.8+3.6% |

cobalt rod at site C18. The flux at this site was reduced by 6.7%, which is about half the average reduction of fluxes at the other 18 sites (13.4%). In general, it is observed that the higher the steam bubble density, the larger the flux reduction around the loop test section, due to the larger neutron absorption by the light water steam. On average, the

thermal fluxes for the 18 sites around the loop test section are reduced by 13.4% and 15.8% for the steam bubble densities of 2 kg/m³ and 10 kg/m³, respectively.

Table 5 shows the comparisons of the seven fuel rod channel powers at sites within two lattice pitches around the E20 loop test section, for cases with and without steam. The rod powers are listed in columns 3 and 5 for steam bubble density of 2 kg/m³, and 10 kg/m³, respectively. The percent changes are listed in columns 4 and 6.

In Table 5, all channel powers for the seven fuel sites with steam are reduced. The site that was least affected was site C18, which is next to a neighbouring cobalt absorber rod site. From the last section, the flux level for this rod is low, so is the rod power, and, therefore, its percent reduction in power is also less. In Table 5, it is observed that the higher the steam bubble density, the larger the power reduction for fuel sites around the loop, because of the larger neutron absorption by steam. For steam bubble densities of 2 kg/m³ and 10 kg/m³, the average channel power of the seven fuel sites around the E20 loop was reduced by 11.5% and 14.6%, respectively.

Table 5 Comparisons of fuel rod powers for sites with steam and without steam.

| Sites (fl=NRU driver Fuel) | Rod Powers With No Steam, MW | Rod Powers With steam, Density = 2 kg/m ³ MW | Percent Change | Rod Powers With steam, Density = 10 kg/m ³ MW | Percent Change |
|-------------------------------------|---|--|-------------------|---|-------------------|
| C18 (fl) | 0.52 | 0.489 | -6.0% | 0.47 | -9.6% |
| D17 (fl) | 1.426 | 1.275 | -10.6% | 1.233 | -13.5% |
| D19 (fl) | 0.892 | 0.785 | -12.0% | 0.753 | -15.6% |
| D21 (fl) | 1.537 | 1.378 | -10.3% | 1.311 | -14.7% |
| E18 (fl) | 1.079 | 0.920 | -14.7% | 0.892 | -17.3% |
| F19 (fl) | 0.936 | 0.787 | -15.9% | 0.766 | -18.2% |
| G22 (fl) | 1.082 | 0.965 | -10.8% | 0.941 | -13.0% |
| Average: | | | -11.5+3.0% | | -14.6+2.7% |

4. Conclusions

In an accident scenario of a coincident pressure tube and liner tube rupture, thermal-hydraulic analysis predicts the formation of a steam bubble of 50 cm radius in the D₂O moderator/coolant around the loop test section. The effect of the steam displacement of the D₂O moderator has been assessed. Several conclusions can be drawn from this study:

- 1) TRIAD3 calculation results show a negative reactivity effect in the NRU core when a steam bubble of 50 cm radius forms at the horizontal mid-plane of the loop test section as a result of a pressure tube crack. The displacement of the D₂O moderator by steam reduces the moderation effect and increases the thermal absorption cross section of the rod assemblies that are occupied by steam.

- 2) This negative reactivity effect is large enough to overcome the positive loop void reactivity (-2.91 mk vs. +2.75 mk) even for the case of a low steam bubble density of 2 kg/m^3 , such that the reactor is shut down and reactor safety is not compromised.
- 3) There are also reductions in fluxes in the 18 neighbouring sites around the E20 loop, 13.4% and 15.3 % for steam bubble densities of 2 kg/m^3 and 10 kg/m^3 . The reductions in the thermal neutron fluxes increase with steam densities.
- 4) Similarly, the rod power reductions in the seven neighbouring fuel rod sites around the loop test section increase with steam densities. The reductions are 11.5 % and 14.6 % for the steam bubble densities of 2 and 10 kg/m^3 , respectively.

5. References

- [1] D.T. Nishimura, "Summary of Loops in Chalk River NRX and NRU Reactors", AECL Report, AECL-6980, 1980 December.
- [2] M. Shams, N. Washba, F. Doria, Y. Parlattan, C. Westbye, and A. Grace, "TUBRUPT-IST V.1.0, Theory Manual", AECL Report, TTR-663, Vol. 2, Rev. 0, 2001 October.
- [3] T.C. Leung and M.D. Atfield, "Validation of the TRIAD3 Code Used for the Neutronic Simulation of the NRU Reactor", Proceedings of the 30th Annual Conference of the Canadian Nuclear Society, Calgary, Canada, 2009 June.
- [4] J.D. Irish and S.R. Douglas, "Validation of WIMS-IST", Proceedings of the 23rd Annual Conference of the Canadian Nuclear Society, Toronto, Canada, 2002 June.

Appendix A: TRIAD3 Neutronic Simulation Code for NRU

The TRIAD3 code was developed in the mid-1980s to perform various physics calculations for the NRU reactor, including core power calculations for determining burnup and depletion in the assemblies in the reactor, reactivity calculations for determining rod shuffles for on-power refueling, control rod worths, reactivity worth of voiding the coolant in a loop, and fast neutron flux levels in material specimens inside fast neutron rods [3]. In the present TRIAD3 code version, 301 rod sites are modeled. In the radial direction, each hexagonal cell is modeled as 6 triangular prisms. In the axial direction, a total of 18 planes, each of variable cell height to match the fuel lengths of the various rod types in the reactor, are used. There are a total of $6 \times 301 \times 18$ triangular prisms (or meshes) for the whole reactor.

The NRU reactor consists of many different types of rods, such as driver fuel rods, fast-neutron rods, Mo-99 production rods, loop fuel strings (for advanced fuel bundle testing), absorber rods and control rods. The 18 axial cells representing a rod in NRU can be of

different types, but each cell type has the same uniform neutronic properties. The detailed flux shapes and neutron spectrum through each type of cell are determined using the WIMS-AECL neutron transport code [4]. The homogenized cell parameters, in two energy groups, are then calculated by flux- and volume-weighting the region material properties. Examples of cell parameters are diffusion coefficients and various cross sections, such as absorption, removal and fission.

After the cell parameters are calculated, the flux and power distributions for the cells in the NRU core can be determined using a modified neutron diffusion theory. The modification is the use of cell discontinuity factors (*cdf*) to improve the radial neutron leakage calculation between adjacent cells. The usual inter-cell leakage calculation in the finite-difference diffusion theory uses a simple linear model, which distorts the flux distribution except in relatively uniform reactors. Since the NRU reactor is made up of many different types of rods, some with very different neutronic properties, it is necessary to use *cdfs* in TRIAD3 to adjust the neutron current calculation at the homogeneous cell boundaries to minimize these distortions. The *cdf* is calculated from the ratio of the heterogeneous to homogeneous cell boundary flux. The heterogeneous cell boundary flux is determined from the WIMS-AECL flux shape by extrapolating the last three mesh point fluxes inside the boundary of the actual cell. The homogeneous cell boundary flux is determined from the boundary flux of a cell having the uniform homogenized cell parameters throughout the cell.

In the TRIAD3 code, the two-group diffusion equations in three dimensions are solved numerically using a finite difference method. The difference equations for the group fluxes in each triangular prism of an NRU hexagonal cell are solved using flux iteration techniques, and to accelerate the flux convergence process successive point over-relaxation is used. After the fluxes in all prisms are determined, the flux in a hexagonal cell is calculated from the average of the fluxes of the six triangular prisms for that cell. The power generated from a hexagonal cell is calculated from the product of the cell flux, the cell volume and the *Q* value, which is the linear heat rating per unit flux per unit cell volume.